

Coupled neutronics and thermal-hydraulics numerical simulations of a Molten Salt Fast Reactor (MSFR)

A. Laureau^{1*}, P.R. Rubiolo¹, D. Heuer¹, E. Merle-Lucotte¹, M. Brovchenko¹

¹LPSC-IN2P3-CNRS / UJF / Grenoble INP, 53 rue des Martyrs, F-38026 Grenoble Cedex, France

*axel.laureau@lpsc.in2p3.fr

Coupled neutronics and thermalhydraulic numerical analyses of a molten salt fast reactor are presented. These preliminary numerical simulations are carried-out using the Monte Carlo code MCNP and the Computation Fluid Dynamic code OpenFOAM. The main objectives of this analysis performed at steady-reactor conditions are to confirm the acceptability of the current neutronic and thermalhydraulic designs of the reactor, to study the effects of the reactor operating conditions on some of the key MSFR design parameters such as the temperature peaking factor. The effects of the precursor's motion on the reactor safety parameters such as the effective fraction of delayed neutrons have been evaluated.

KEYWORDS: *coupled neutronics and thermalhydraulic analysis, CFD, Monte Carlo, Molten Salt Fast Reactor*

I. Introduction

Molten Salt Reactors (MSRs) are one of the reference nuclear systems identified by the Generation-IV International Forum (GIF). Since 2004, the National Centre for Scientific Research (CNRS, Grenoble-France) has focused R&D efforts on the development of a new MSR concept called the Molten Salt Fast Reactor (MSFR) [1-3]. As opposed to thermal molten salt reactors, the MSFR does not employ any solid moderator (such as graphite) in the core which results in a fast-spectrum breeder reactor with a large negative power coefficient that can be operated in a Thorium fuel cycle. Other advantages of a fast spectrum MSR include the reduction of the reprocessing requirements, the better reactor breeding ratio, and the absence graphite lifespan issues. These unique advantages for actinide burning and extending fuel resources have been recognized by the GIF forum which selected the MSFR concept in 2008 as one of the GEN IV reference reactors [4].

One key characteristic of a Molten Salt Reactor is the use of a flowing liquid fuel which also serves as coolant for heat transport from the core to the intermediate loop heat exchangers. The neutronics and thermohydraulics design of such a reactor have then some important differences with respect to nuclear power system using a solid fuel. In particular, some unique phenomena caused by the circulation of the liquid fuel in the reactor have to be integrated in the analysis. These phenomena include: the motion of the delayed neutron precursors, the fuel irradiation which depends on the salt circulation, the coupling between salt temperature distribution and the reactivity feedback, the reactor core wall temperature distribution, etc. Coupled neutronics and thermohydraulics numerical simulations are thus necessary to adequately take into account these phenomena. Moreover, due to the complexity of the flow

distribution in the core, one dimensional flow models such as the commonly used subchannel approaches do not provide enough accuracy.

This work presents an approach based on coupled numerical simulations using the Computational Fluid Dynamics (CFD) code OpenFOAM version 2.2.0 [5] and the Monte Carlo code MCNP version 5 [6]. The main objectives of this preliminary analysis are to confirm the acceptability of the current neutron and thermal-hydraulics designs of the reactor, and to better evaluate the effect of the precursor's motion on the reactor safety parameters. Medium term objectives of the numerical model include performing selected transient studies for normal or incidental conditions, studying the reactor materials solicitations due to the temperature and irradiation fields, etc.

II. System description

The reference MSFR design is a 3000 MWth reactor with three different circuits (or loops): the fuel circuit, the intermediate circuit and the power conversion system. The main components of the fuel circuit are: the fuel salt which serves as fuel and coolant, the core cavity, the inlet and outlet pipes, the gas injection system, the salt-bubble separators, the fuel heat exchangers and the pumps. The molten salt in the fuel loop is composed by a mixture of a lithium fluoride and thorium fluoride salts with a proportion of heavy nuclei fixed at 22.5%. The total fuel salt volume in the fuel loop is about 18 m³ and the mean salt temperature of about 675°C. As shown in the sketch of Figure 1, the fuel salt flows from bottom to the top of the core cavity. After exiting the core, the fuel salt is fed into 16 groups of pumps and Heat Exchangers (HXs) located around the core. The fuel salt circulates in the fuel circuit in around 3-4 seconds. Three important components of the core are: i) the upper and

lower axial neutron reflectors and ii) the radial fertile blankets (shown in red in Figure 1) which is part of the radial reflector and allows increasing the MSFR breeding ratio. This blanket is filled with a fertile salt of LiF-ThF₄ with initially 22.5 mole % ²³²ThF₄. The fuel circuit includes a salt draining system which can be used for a planned shut down or in case of incident/accident leading to an excessive increase of the temperature in the core. Another important reactor component is the fuel reprocessing units. Fuel salt cleaning [7] involves two processes: 1) the mechanical extraction of rare gases and some noble metal via an on-line bubbling process in the core; 2) the removal of other fission products via batch reprocessing of small fuel salt sample at an on-site chemical reprocessing unit near the reactor. Thanks to the MSFR fast spectrum, this unit only extracts a small amount of the fuel salt (order of a few liters per day) for fission product removal and then returned to the reactor. This is important difference with thermal molten salt concepts which usually requires very large reprocessing salt volumes.

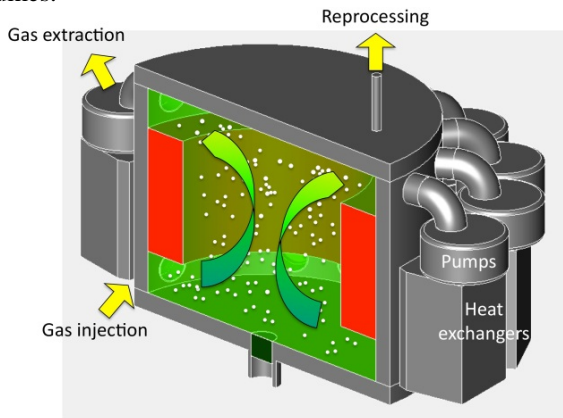


Figure 1: Schematic layout of the Molten Salt Fast Reactor (MSFR) fuel circuit

III. Methodology

In order to take into account the phenomena associated to the fuel salt circulation, an approach based on coupled neutronics and thermal-hydraulics numerical simulations is used. The Computational Fluid Dynamic code OpenFOAM is employed to predict the fuel salt velocity distribution, the neutron precursors concentration and the temperature distributions in the salt and on the fuel loop walls. The Monte Carlo code MCNP is used to predict the fission power distribution in the salt and to determine the reaction rates in the different mechanical components of the reactor.

The geometry domain covered by the simulations includes the main fuel circuit components such as the core cavity, the inlet/outlet legs and Heat Exchangers (HXs). The fuel salt pumps were not explicitly modeled but take into account as imposed pressure rise in the circuit. The MSFR bubbling system used for fission product reprocessing is neither considered in the analysis since under most normal and abnormal conditions it impact on the salt flow can be neglected. Figure 2 shows the 3-D geometry used in the study. As can be seen in this figure, the core cavity is rather complicated component since it has curved radial walls and

also inlet and outlet legs. These particular features allow improving the fuel salt flow mixing in the core and thus decreasing the temperature hot-spots on the core walls. In these preliminaries studies a one-sixteenth core model was used in order to reduce the computational effort. A larger one-quarter model will be used in the future to allow performing studies on the reactor flow conditions after the stop of a fraction of the fuel salt pumps or to investigate the presence of flow structures (steady or unsteady) involving several loops.

Approximations involving steady turbulent fuel salt flow conditions and constant nuclear power generation are used in the current analysis. As previously discussed, the fission source was determined using the Monte Carlo N-Particle code (MCNP).

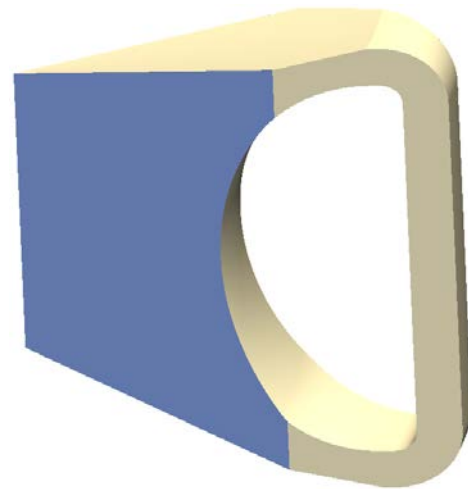


Figure 2: 3-D geometries of a one-sixteenth of the MSFR fuel circuit used in the coupled studies

1. MSFR thermalhydraulics core model

The model equations were solved assuming that steady turbulent flow conditions exist in the reactor. This is indeed the case in many practical situations (and also suitable for the MSFR), where the flow is steady in the mean; i.e. while unsteady turbulent fluctuations exist, the time averaged velocity field appears to be steady. The numerical resolution of the flow mass, linear momentum and energy balance equations was carried out in two different manners: i) using steady simulations which neglect the governing equations' time derivatives and ii) performing a transient simulation which takes into account the equations' time derivatives. Since the problem variables (reactor thermal power and boundary conditions) are assumed to have a constant value, both approaches should in principle converge to the same solution provided that truly turbulent steady conditions exist. The results of the simulations seem to support this assumption since the presence of flow instabilities (transient flow) can be detected sometimes because of the poor numerical convergence of the CFD simulations that they cause. This was not the case of the simulations presented in this paper since a good convergence was found thus supporting the assumption of steady turbulent flow conditions for the two proposed geometries. On the contrary, in other geometries (not discussed here) a bad numerical

convergence was sometimes observed which may indicate the existence of flow transients. At a more advance phase of the reactor design, it would be suitable to perform transient calculations using a more detailed description of the reactor (for instance including the detailed HX's design). At the present stage, where various core geometries were investigated, this will be prohibited.

i) Conservation of mass, linear momentum and energy

Assuming a constant salt density ρ_o the averaged mass conservation equation (continuity equation) is simplified as follows:

$$\frac{\partial \bar{u}_j}{\partial x_j} = 0 \quad (1)$$

In the case of steady turbulent flow then \bar{u}_j is the time averaged value of the j component of the fuel salt velocity. If the flow is not turbulent steady (transient flow), the time averaging has to be replaced by the ensemble averaging. As can be seen in Table 1, the salt density varies in function of the temperature. However, the constant salt density approximation (thus incompressible flow) still provides a good accuracy for our applications as long as the effects of the fuel salt density variations in the gravity force are taken into account through the Boussinesq approximation.

The momentum conservation equations were solved using the Navier Stokes equation with the turbulence Realisable k-epsilon model:

$$\begin{aligned} \frac{\partial \bar{u}_j}{\partial t} + \frac{\partial}{\partial x_j} (\bar{u}_j \bar{u}_i) = & -\frac{\partial}{\partial x_i} \left(\frac{\bar{p}}{\rho_o} + \frac{2}{3} k \right) \\ & + \frac{\partial}{\partial x_j} \left\{ (v + v_t) \left[\left(\frac{\partial \bar{u}_i}{\partial x_j} + \frac{\partial \bar{u}_j}{\partial x_i} \right) - \frac{2}{3} \left(\frac{\partial \bar{u}_k}{\partial x_k} \right) \delta_{ij} \right] \right\} \\ & + g_i [1 - \beta (\bar{T} - T_o)] \end{aligned} \quad (2)$$

where \bar{p} is the time averaged fluid pressure, v the kinematic viscosity, v_t the turbulent viscosity, g_i the i component of the gravity acceleration, k the turbulent kinetic energy, β the salt expansion coefficient, \bar{T} the salt time averaged temperature and T_o a reference temperature (for example the inlet temperature). The equation uses the Boussinesq approximation, i.e. only the gravitational force takes into account the effects of the density variation through the salt expansion coefficient. Both v_t and k are calculated according to the turbulence Realisable k-epsilon model whose characteristics can be found in the literature [8]. At the current stage of the MSFR design, a « RANS » model (Reynolds Average Navier Stokes) provides a good compromise between the precision required for the thermal-hydraulics design, the computational effort and the number of scoping studies that are needed. Moreover, some prospective studies have confirmed that for Reynolds number over 50000, the results precision of Realisable k-epsilon model is quite good. During the next stage of thermal-hydraulics studies a more precise turbulence model such as a LES approach and a comparison against an

experimental benchmark would be suitable.

Without introducing a significant error, and assuming incompressible flow, the fuel salt energy conservation equation can be approximated as follows:

$$\frac{\partial \bar{T}}{\partial t} + \frac{\partial}{\partial x_j} (\bar{T} \bar{u}_j) = k_{eff} \frac{\partial}{\partial x_k} \left(\frac{\partial \bar{T}}{\partial x_k} \right) + S \quad (3)$$

where \bar{T} is the salt time averaged temperature and

$$k_{eff} = \frac{v_t}{Pr_t} + \frac{v}{Pr} \quad (4)$$

The salt Prandtl number Pr and other salt thermodynamic properties are calculated using the correlations for the fuel salt. The turbulent Prandtl number Pr_t is determined from the turbulent viscosity and conductivity which are computed from k-epsilon equations. The energy released by the fission reaction and the decay heat from the fission products and actinides is represented by the volumetric heat source number S . Under steady reactor operation, the heat source S depends only on the spatial position and is determined from the MCNP neutronic simulations as discussed in the next section.

ii) Boundary conditions

In the current simulations, the CFD model domain includes the entire fuel circuit geometry (i.e. it is a close loop). Without introducing too much error, the HXs are modeled as pipes with a volumetric impulsion force in the fluid to obtain the nominal flow rate in the reactor medium and thus approximating the presence of the fuel salt pumps. As already discussed, the MSFR bubbling system used for fission product reprocessing is not considered in the analysis since under most of the normal/abnormal conditions its effects on the salt flow are negligible. The following conditions were used in the simulations:

(a) Core operating conditions

- The total flow rate is equal to 18932.2 kg/s (for the full core) which corresponds to 1183.3 kg/s in each loop. The pump impulsion was adjusted such as obtaining the appropriate loop flow rate in the leg.
- The inlet core fuel salt temperature was setup equal to 625°C which provides an approximate core mean temperature of 675°C consistent with the salt temperature used in neutronics calculations.

(b) Bottom and top reflectors and blanket walls:

- Non-slip conditions with a wall function for turbulence model that assumes a small wall roughness (which corresponds to an hypothesis of a roughness height smaller than 40-50 micron).
- Adiabatic wall (no heat flux). As previously discussed, the blanket heat source is about 25 MW and thus negligible with respect to the 3,000 MW source in the core. Therefore the blanket heat source does not significantly contribute to heat up the salt flow in the

core. For the top and bottom reflectors, the adiabatic wall assumption implies that the heat leak is negligible compared to the total power. This assumption is conservative since they will lead to a slightly overestimate of the wall temperature.

iii) Fuel salt thermodynamic properties

Consistently with the current MSFR configuration, a binary fluoride salt, composed of LiF enriched in ^7Li to 99.995 mol % and 22.5 mol % of heavy nuclei has been used as

working fluid in the CFD simulations. While during reactor operation, fission products and new heavy nuclei are produced in the salt up to some few mol %, they do not impact the salt thermodynamic properties used in these studies. The fuel salt properties are considered then as unchanged over time and equal to those of the initial fuel load. The experimental determined correlations employed to calculate these properties are given in Table 1. The fuel salt melting temperature is equal to 838 K (565°C).

Property	Units	Equation	A	B	Temperature validity range
Specific heat capacity [C_p]	J/K/kg	A+BT	-1111	2,78	[867 K - 907 K]
Thermal Conductivity [λ]	W/K/m	A+BT	0.928	8.40E-05	[891 K – 1020 K]
Density [ρ]	kg/m ³	A+BT	4983.56	-0.882	[893 K – 1123 K]
Dynamic viscosity [μ]	Pa.s	$\rho \cdot A \cdot \exp(B/T)$	5.55E-08	3689	[898 K – 1119 K]

Table 1: Fuel salt thermodynamic properties used in the analyses [9]

iv) CFD Model mesh

The mesh characteristics were chosen to obtain a good balance between convergence and precision (of the temperature and velocity gradients), and the computing effort. At this stage of the reactor design, this last constraint is important since various core geometries have to be investigated. The maximum bulk cell size is comprised between 2 and 3cm, with a refinement near the core walls with reduce the cell thickness to about to 2 mm. In order to decrease the number of cells a mesh technique by elevation was used: the mesh algorithm created hexahedra from quadrangle surface elements, and prism from triangle surface elements. The full 3D meshes of a quarter of the core contain between 1 million cells. The mesh used is illustrated in figure 3.

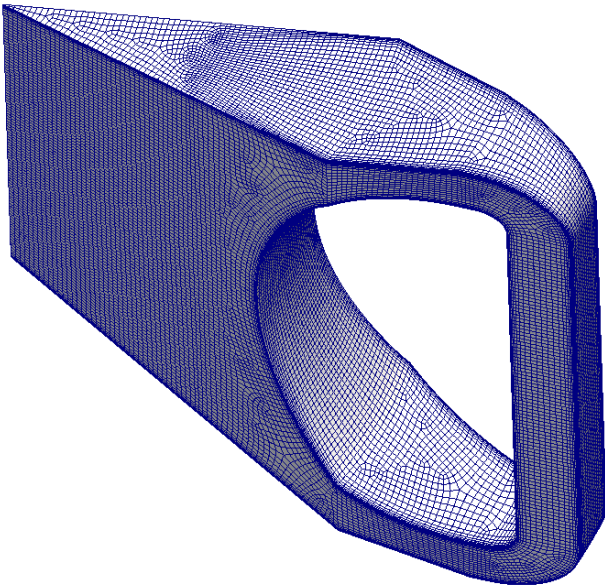


Figure 3: Example of the CFD mesh used in the thermal-hydraulics studies

v) CFD code

In the present analysis, the CFD code OpenFOAM (Open source Field Operation And Manipulation) was employed to predict the fuel salt velocity and temperature fields. OpenFOAM [5] is a free and open source only toolbox that allows developing numerical solvers, and pre-/post-processing utilities for the solution of computational fluid dynamics.

2. MSFR neutronics model

i) Neutron transport

The neutron flux in the reactor can be accurately predicted by solving the Boltzmann equation:

$$\frac{1}{V} \frac{\partial \varphi}{\partial t} + \vec{\Omega} \cdot \nabla \varphi + \Sigma_t \varphi = \frac{\chi_p}{4\pi} \int_0^\infty dE' v_p(E') \Sigma_f(E') \varphi(E') + \sum \frac{\chi_{di}}{4\pi} \lambda_i C_i + \int_{4\pi} d\vec{\Omega}' \int_0^\infty dE' \Sigma_s(E' \rightarrow E, \vec{\Omega}' \rightarrow \vec{\Omega}) \varphi(E', \vec{\Omega}') \quad (5)$$

where $\varphi(\vec{r}, E, \vec{\Omega}, t)$ is the neutron angular flux, V the neutron velocity, $v_p(E)$ the average of prompt neutrons produced per fission, $\vec{\Omega}$ the neutron direction, Σ_t the total macroscopic cross section, Σ_f the fission macroscopic cross section, χ_p the prompt neutron energy spectrum, χ_{di} the energy spectrum of the delayed neutron group i , $C_i(\vec{r}, t)$ neutron precursor group i concentration at the position \vec{r} and time t , and λ_i the group i decay constant. The numerical resolution of equation (5) is complicated but can be performed using a deterministic approach to discretize the neutron flux.

A rather different approach to compute neutron transport consists in using a stochastic approach which does not solve the transport equation but rather compute a large number of neutrons histories in order to estimate a global behavior from which correspond to the neutron flux in each position of space. By computing the neutron histories, the stochastic

code can determinate the neutrons induced fissions from which one can be determined the precursors generation rate (in our analysis we consider 7 different families each with a different relative abundance β_i). As previously mentioned, in a molten salt reactor, the motion of the salt induces the motion of these precursors. Indeed precursors can be treated as chemical species transported by the fluid. Some of the groups of neutron precursors have decay constant (up to 50 s) that can be much higher than the circulation time of the salt in the core (3-4 s) while others are significantly shorter thus having a different final impact on the neutron flux and the reactor reactivity. This phenomenon has to be taken into account in order to evaluate the flux shape deformation.

ii) Impact of the precursor motion

In this section, the objective is to estimate with MCNP the contribution of the precursor motion on some of the results of interest for our analysis (e.g. the effective fraction of delayed neutrons). Indeed, due to the motion of the precursors, their final decay position is different from their initial creation position.

Stochastic calculation codes like MCNP are modeling critical systems by tracking successive generations of a certain amount of neutrons (called cycles, or batches). For each cycle, the sources distribution is the fission distribution obtained in the previous cycle. From those cycles, different key neutronics parameters can be estimated, such as the k_{eff} (multiplication factor), the neutronic flux and the energy deposition.

This method allows calculating the equilibrium flux for a static fuel material but can still be used in system such as in the MSFR where the fuel circulates in the core (and thus the precursors can enter and exit the core) by introducing some modifications. First in a critical system ($k_{eff} = 1$) the reactor can be considered as a prompt subcritical system with an exterior neutron source created by the delayed neutrons. Since the system is critical (and thus steady-state), then the prompt neutron multiplication factor k_p is smaller than 1 and each chain-reaction induced by a prompt neutron population will die after a certain number of generations (the delayed neutrons being not taken into account in this argumentation). By considering the core as a prompt subcritical system it follows that the neutron flux is obtained by the amplification of the source, i.e. the delayed neutrons originated by the decay of the neutron precursors. Therefore, at the equilibrium all neutrons in the core can be linked to a descendant of a precursor's decay.

Using this idea, one can estimate the prompt neutron multiplication factor and the neutron flux as follows [10]:

$$\phi = \phi_1 + k_1^p \phi_2 + k_1^p k_2^p \phi_3 + \dots + \left(\prod_{m=1}^{m_0-1} k_m^p \right) \phi_{m_0} + \left(\frac{\prod_{m=1}^{m_0} k_m^p}{1 - k_{eff}^p} \right) \phi_{eff} \quad (6)$$

Where k_i^p is the prompt multiplication factor of the generation i and $\phi_i(\vec{r}, E, t)$ the neutron flux calculated for this generation. For each generation, the number of neutron generated is the same. Thus the flux calculated for each generation can not be directly aggregated, but weighted by the k_i^p between generation i and $i+1$.

ϕ_1 represents the flux of the first generation of neutron created by the decaying neutron precursors. The distribution of the concentration of the neutron precursors is calculated from the thermal hydraulics analysis discussed in the previous section. This precursor distribution is thus used then to generate the source distribution of the first generation.

The first terms, from 1 to m_0 , are calculated using MCNP with a calculation without cycle discarded. Note that during the simulation, a high number of neutrons per cycle will be required in order to have a good convergence for each cycle. To evaluate equation (6), each generation contribution has to be extracted from MCNP output. It is possible in MCNP to print the tally estimators for each cycle by using the "prdm 1" card. From MCNP, tallies are normalized by the number of source particles, and this number increases after each cycle. The value of the contribution of the generation i to the tally value can be deduced by multiplying the number of sources used for the i generation, minus the tally value for the $i-1$ generation multiplied by the number of sources of the $i-1$ generation.

The final term ϕ_{eff} represents the equilibrium flux, without the precursor influence. It is estimated in MCNP with a "classical" calculation discarding the first cycles in order to have a converged source distribution.

Two MCNP calculations are necessary to evaluate the equation (6): one simulation with which all the tallies are printed for each cycle, without discarding any generation; and one simulation to calculate the equilibrium value of tallies using a discard of the first cycles.

iii) Estimation of the effective fraction on delayed neutron $\tilde{\beta}$

The objective of this part is to estimate the safety margin to the prompt criticality: $1 - k_p = \tilde{\beta}$ at equilibrium.

As explained previously, all the neutrons in the core at equilibrium are descendants of a precursor decay.

Then the equilibrium condition assumes that one neutron source coming from the precursor distribution generates, statistically, one precursor. Then the quantity:

$$\beta v \Sigma_f \phi = \beta v_1 \Sigma_f \phi_1 + k_1^p \beta v_2 \Sigma_f \phi_2 + k_1^p k_2^p \beta v_3 \Sigma_f \phi_3 + \dots + \left(\prod_{m=1}^{m_0-1} k_m^p \right) \beta v_3 \Sigma_f \phi_{m_0} + \left(\frac{\prod_{m=1}^{m_0} k_m^p}{1 - k_{eff}^p} \right) \beta v_{eff} \Sigma_f \phi_{eff} \quad (7)$$

must be equal to 1 for the system at the equilibrium.

This quantity can be estimated using MCNP and adjusted to

one by modifying the fissile proportion.

In this case, the system is at equilibrium and the influence of the precursor motion on the neutron losses outside of the critical zone is taken into account. For this fissile proportion, a KCODE calculation with discard would lead to an $k_{eff} > 1$. Indeed some neutrons are lost by the precursor motion and the "real" effective multiplication factor is 1. The k_p estimator would correspond to the real k_p of the core at equilibrium, taking into account the precursor motion.

Then the safety margin to the prompt criticality is estimated as $\beta = 1 - k_p$. An estimation of β is realised in the results part.

3. Coupling strategy

i) Data exchange strategy between codes

In this analysis the neutronics and the thermal hydraulics behaviors of the fuel salt are studied, therefore the computing domain (see for example Figure 2) is the same for both OpenFOAM and MCNP. The fuel salt geometric can be designed with the help of the ANSYS design modeler. This tool can export a simple geometry (including torus) as an MCNP input file. In this way, it is possible to create a surface description of the reactor limits for MCNP corresponding exactly to the CFD geometry and avoid potential mapping problems. A slightly simplified version of the actual MSFR core design [11] was developed with ANSYS design modeler. The geometry used in the current studied is therefore not fully optimized for some CFD aspects like reducing the hotspots on the wall.

From the MCNP input file exported from the ANSYS design modeler, a complete geometry is generated in order to have a spatial discretization (maximum cell size) of approximately 6cm (~5000 cells, see Figure 4). The program used to generate the MCNP input file enables to map¹ data between the CFD mesh (~300 000 cells) and MCNP's volumes. For simplicity and without losing precision, to map a scalar field (e.g. temperature) from one spatial discretization to the other, each cell of the CDF code is considered as a node and corresponding to only one volume of MCNP.

In the following studies, tallies values are integrated values over volume of MCNP's geometry. Indeed the volume value given to MCNP to normalize tallies is 1 for each MCNP's volume. The volumes of MCNP's cells are estimated with a statistic approach using MCNP due to the complexity of the surfaces: cylinder portion cut by torus. Before mapping the value to OpenFOAM, the tally is divided by the volume estimated in a previous distinct calculation to obtain the corresponding intensive values.

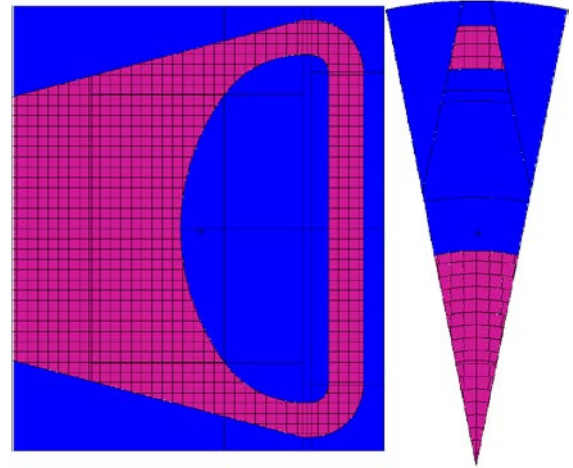


Figure 4: MCNP geometry (magenta: fuel salt / blue: Ni-based alloy)

The result of interest obtained in this study is the steady state solution of the neutronic / thermal hydraulics coupling. The neutronic power is normalized to 3GW/16 for the CFD code (one-sixteenth of the MSFR fuel circuit is modelised) from the energy deposition field estimated by MCNP using equation (6). At steady-state conditions, there is no need for a neutronic calculation at each time step of the thermal hydraulic transient calculation (~ 1 μs). The neutronics calculations can then be performed every 5-10 s (of the thermohydraulic transient) due to the weak impact of the shape of the temperature distribution (and precursor's concentration distribution) on the shape of the flux distribution and vice versa. During a transient calculation this constraint will be much more restrictive. The steady-state coupling schema is given in Figure 5. Finally, to speed-up the convergence of the precursor concentration distribution, their concentration value is initialized to the equilibrium volumetric value on the whole core. In this way, the convergence of the precursor distribution is only linked to the thermal-hydraulics and to the power distribution, and not to the temporal accumulation of the precursors.

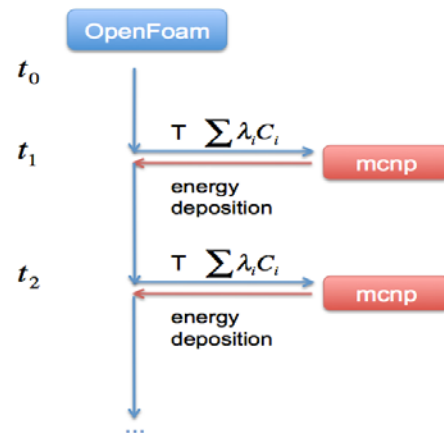


Figure 5: Coupling scheme

¹ Mapping: data transfer between different meshes

ii) Statistical convergence

In order to estimate the statistical error of the MCNP tallies, sixteen different calculations are performed with different random seeds. The standard deviation is calculated for each cell (volume) of MCNP's geometry using:

$$\sigma_{cell} = \frac{1}{\bar{t}_{cell}} \sqrt{\frac{1}{nb_{simulation}} \sum_{j=1}^{nb_{simulation}} (t_{cell_j} - \bar{t}_{cell})^2} \quad (8)$$

Where t_{cell_j} is the tally value of MCNP for the simulation j , the tally corresponding to the energy deposition or the neutron production for this study. \bar{t}_{cell} represents the mean value of the different simulations.

In Figure 6 is displayed the number of cells as a function of the corresponding standard deviation of the energy deposition (calculated from MCNP's tally F6). If $\sigma_{cell} > 1$, the value is put to 1. Two cases are studied: 2 000 and 20 000 neutrons per cycle with 300 discarded cycles and 1200 active cycles. The median value is equal to 0.028 for 2.4 million of actives particles, and 0.008 for 24 million (see Figure 6).

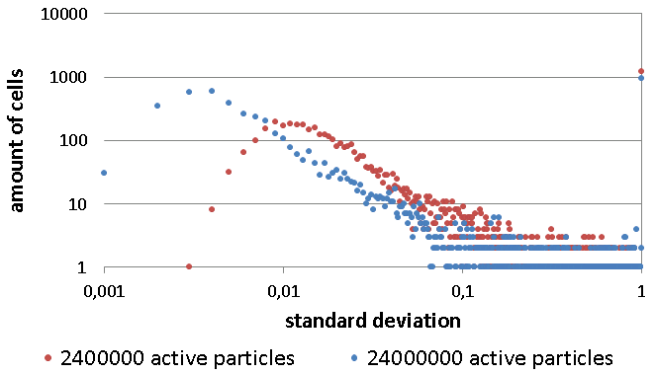


Figure 6: Distribution of the amount of cells as a function of the standard deviation for different statistical convergences

As can be seen in Figure 6 about 1000 MCNP's cells have a $\sigma \geq 1$. This is explained by the fact that those cell volumes do not accumulate enough statistics during the MCNP simulations. Indeed, a fraction of the sources (decaying precursors) are located in these low flux areas. To investigate this point, high-error - low-flux, the standard deviation versus the relatively flux and the number of cells is plotted in Figure 7. As can be seen from the figure the largest errors correspond to the cells having the lowest flux. Only the volumes with high flux have a significant influence on the thermal hydraulics, while low flux volumes have a lower importance on the result. Even if a part of cells have a high error, those cells don't have a huge impact on the thermal hydraulics.

An estimation of the standard deviation of the whole simulation can be estimated with:

$$\langle \sigma_{cell} \rangle = \frac{1}{\sum_{cell} t_{cell}} \sum_{cell} (\sigma_{cell} \cdot t_{cell}) \quad (9)$$

where $cell \in$ MCNP's volumes

We obtain $\langle \sigma_{cell} \rangle = 0.012$ with 2.4 million active particles and $\langle \sigma_{cell} \rangle = 0.0038$ with 24 million active particles. We can conclude that, as expected, the statistical error decreases with the square root of the number of active particles ($\frac{0.012}{\sqrt{10}} = 0.00379$). Then, with the 16 independent simulations used to estimate the standard deviation, the standard deviation of the medium value can be divided by a factor 4. Here we can estimate the global convergence of the flux.

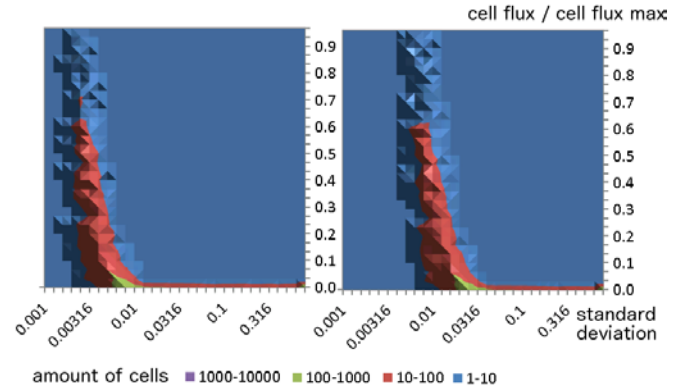


Figure 7: Amount of cells as a function of the standard deviation (abscissa) and of the relative flux (ordinate), left/right: 24/2.4 million active particles

For the calculation of the standard deviation of the flux distribution calculated using the equation (6), the estimation of this distribution is done for each simulation and compared using the same formula.

IV. Results

The results of the thermal hydraulic – neutronic coupling assume that the fissile fuel salt load ensures that the reactor is at critical conditions. Therefore a necessary step in the steady-state calculation is the determination of the fissile load. This can be done at the same time as effective fraction of delayed neutron is estimated.

1. Estimation of the effective fraction of delayed neutron

As previously explained, the objective is to adjust the fissile proportion in the heavy nuclides to obtain the equilibrium condition: one neutron history induced by a decaying precursor produces, statistically, one precursor: this is equivalent to set the equation (7) equal to 1. The neutron creation rate can be estimated in MCNP as the $\nu \Sigma_f \phi$ value. In this way we obtain, for each volume, the neutron production rate per source neutron (precursor decay) integrated on all the generations descending of the sources.

In equation (7), the term with the main impact is the last one ($\sim 96\%$ of the total value near to the criticality with $m_0 = 30$) due to the $\frac{1}{1-k_p}$ term where $1 - k_p$ is going from 100pcm to 1000pcm. Then the dependency of the neutron produced per source can be easily interpolated using an $\frac{A}{1-k_p}$ function where A is a constant. Indeed as we can

see in Figure 8, with $A = 50818$ pcm, the calculations of MCNP and the trend line are in good agreement.

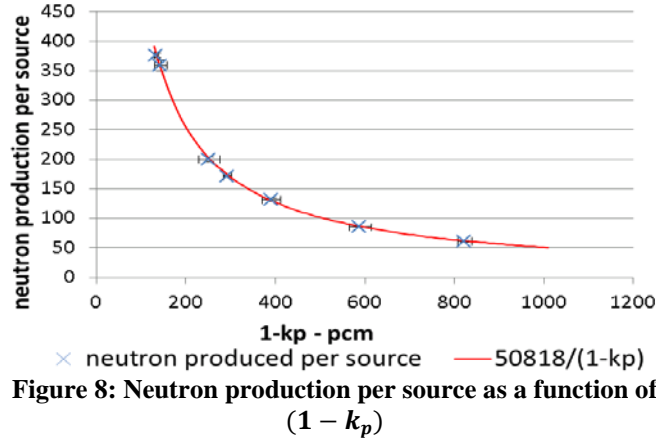


Figure 8: Neutron production per source as a function of $(1 - k_p)$

At this point we have an estimation of the neutron production per source ($n_{prod/src}$) as a function of $(1 - k_p)$.

We are looking for the k_p value by checking $n_{prod/src} * \beta = 1$ where β is the value of the fraction of delayed neutrons fraction: $\beta = \frac{k_{eff} - k_p}{k_{eff}}$. The value of β can be estimated in MCNP by doing an keff estimation with the "TOTNU" card and an k_p estimation using "TOTNU NO" card.

We obtain $\beta = 304 \pm 7$ pcm. The value $n_{prod/src} * \beta$ is the number of precursors produced per source. And then:

$$n_{prod/src} * \beta = 1 \Leftrightarrow (1 - k_p) = \tilde{\beta} = A * \beta$$

We obtain $\tilde{\beta} = 154$ pcm. If we consider the A value as accurate, the standard deviation of $\tilde{\beta}$ is 4 pcm. However the best way to estimate the standard deviation is to do a new calculation with a good statistics for the corresponding fissile proportion (0.11595% atomic).

The $\tilde{\beta}$ value obtain is a bit higher than the value usually obtained [12] for this reactor. Indeed, the geometry is not the usual one. Here the heat exchanger volume is smaller than the volume it is supposed to be, and fewer precursors are decaying in it. Then more precursors are decaying in the core and their importance is overestimated. Modeling a bigger heat exchanger volume or modifying the decay constant in the heat exchanger zone would permit to estimate the good estimation of $\tilde{\beta}$.

2. General results

The results presented in this section were obtained after convergence. It corresponds for the thermal hydraulics transient of 40 "real" seconds equivalent and thus 10 exchanges with MCNP. The statistical convergence was improved by gradually increasing the number of active particles up to 25 millions (multiplied by 16 simulations) for the equilibrium calculation. For the first terms of the equation (7) corresponding to the flux of the m_0 firsts generations, the number of active particles increase up to 1

million of neutrons per cycle (multiplied by 16). The flux distribution can be considered as converged after 30 cycles (m_0) as it will be explained at the end of the section.

The fuel salt velocity field is shown Figure 9. A recirculation can be observed at the bottom of the reactor, next to the toroidal wall. Recirculations are characterized by a reverse flow next to the wall. As have been already mention, the geometry could be further optimized to further reduce the reverse flow in order to minimize temperature hot spots on the wall (see Figure 11).

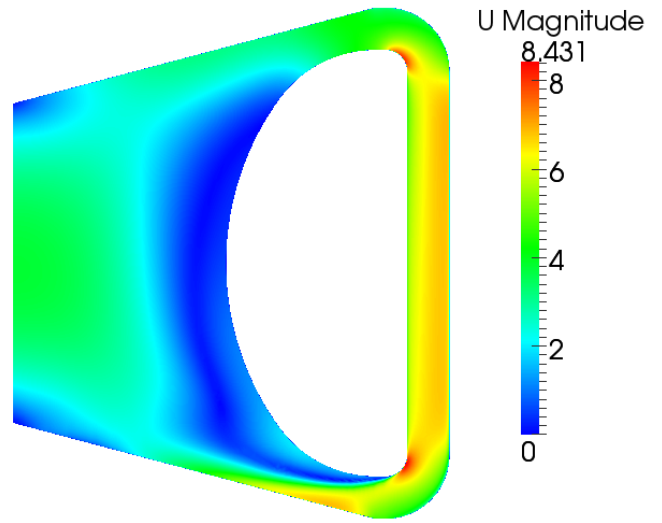


Figure 9: Velocity magnitude field

The salt axial velocity is presented in figure 10 along a line which is placed in a middle plane of the core. The maximum velocity at the center of the cavity is close to 4m/s. Near to the wall, the reverse flow can be observed with the negative velocity along the vertical axis. We can although notice that the non-slip condition on the wall (null velocity) is respected.

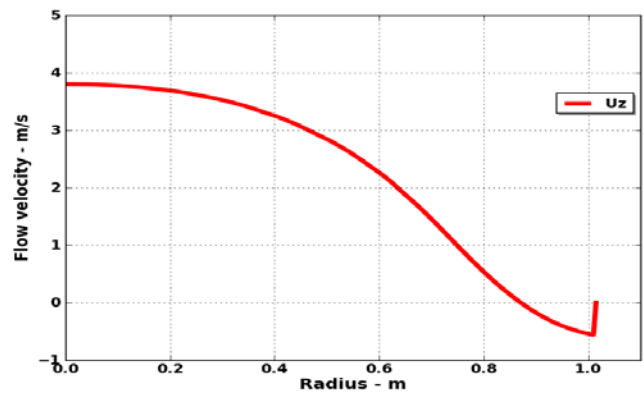


Figure 10: Vertical velocity at the middle plane

In Figure 11 we can observe the temperature field with a hotspot on the radial wall. The temperature field is mapped

from OpenFOAM mesh to MCNP's one. This temperature field is used by MCNP to set the appropriate cross-sections of the volumes and then recalculate the energy deposition. The cross-sections libraries have been previously generated using a temperature step of 10 K with ENDF-B7 library. The temperature of MCNP's volumes have been condensed each 10K and the density recalculated accordingly. The difference of meshing between the two codes will of course slightly change the temperature discretization as can be observed in Figure 11 (the MCNP's meshing is coarser than the one of OpenFOAM). Nevertheless it was found that the effect is negligible.

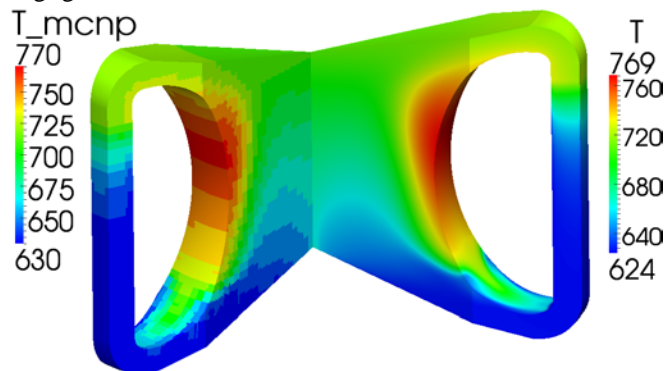


Figure 11: Temperature field in OpenFOAM in °C (right) and mapped back from MCNP (left)

Precursors are generated using the neutron production rate calculated using (7) by decomposing β for each family of precursor β_i . Seven families of precursors are simulated in this study. The precursor concentration is normalized to obtain: $\sum \lambda_i C_i = 1$. An example of precursor concentration corresponding to two families with the extreme decay periods are presented in figure 12. The family 6 (right) has a decay period of 0.199 second. We can observe here that most of the precursors of this family decay in the core. The family 0 (left) has a period of 55.9 seconds. Its accumulation is much more important and its density is quite identical on the whole core.

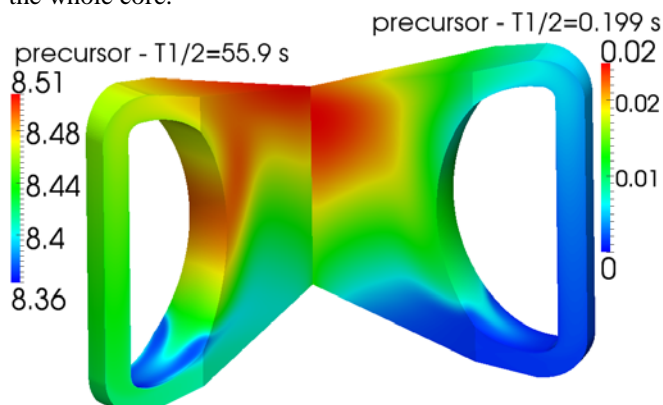


Figure 12: Precursor field for the families 0 (left) and 6 (right) on different scales

The neutron source term for MCNP is deduced from the precursor concentration: $\sum \lambda_i C_i$. The total decaying precursor's distribution source is displayed in figure 13 (left). This field is mapped to MCNP. Each volume of MCNP

contains a Dirac source with the coefficient: $\sum \lambda_i C_i * Cell_{volume}$. For this first approach, the initial energy of the neutrons issued from the precursors is fixed to 0.4 MeV instead of χ_d . The effect of this source is directly visible on the energy deposition of the first cycle (Figure 13, on the right).

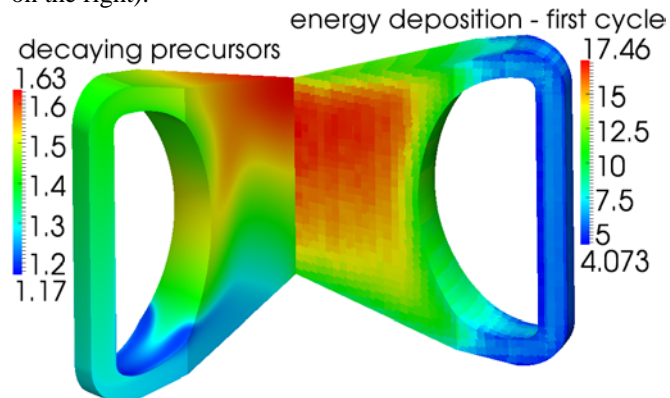


Figure 13: Sum of decaying precursors (left) and energy deposition of the first batch in MeV/source (right)

The flux of the first cycle (corresponding to the first neutron generation) is very different from the one of the equilibrium cycle. It is important to check that the last flux of the generation m_0 is converged. This convergence of the flux can be estimated for each generation i by the standard deviation between the value of simulations and the equilibrium value:

$$\langle \sigma_i \rangle = \frac{1}{\sum_{cell} t_{cell\infty}} \sum_{cell} (\sigma_{cell_i/\infty} t_{cell\infty}) \quad (10)$$

where:

- $cell \in$ MCNP's volumes
- ∞ refers to the equilibrium value
- $\sigma_{cell_i/\infty} = \frac{1}{t_{cell\infty}} \sqrt{\frac{1}{nb_{simulation}} \sum_{j=1}^{nb_{simulation}} (t_{cell_{ij}} - t_{cell\infty})^2}$ (11)

where $t_{cell_{ij}}$ refers to the tally value of the cell for the generation i at the simulation j , and $t_{cell\infty}$ to the tally equilibrium value of the cell.

The evolution of $\langle \sigma_i \rangle$ as a function of the cycle number is drawn in Figure 14. We can directly observe the convergence of the flux distribution over the cycle number. Here, for this critical system with a fast spectrum, this convergence is obtained for ~ 25 cycles. It is a quite low number of cycles, indeed the fast spectrum implies an important migration area and thus a good source convergence.

The energy deposition is drawn in figure 15. Two versions are given here, the "equilibrium" energy deposition with converged sources (classical calculation with a discard of the firsts cycles) on the left, and the energy deposition using the flux calculated with the equation (6) on the right.

These two distributions are extremely similar. Indeed, the last term of the equation (6) is the addition of the

equilibrium flux and represents 96% of the total value.

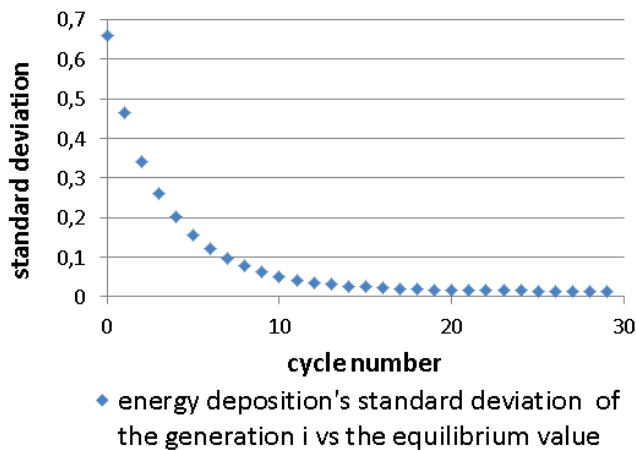


Figure 14: Evolution of the flux matching between the generation i and the equilibrium value

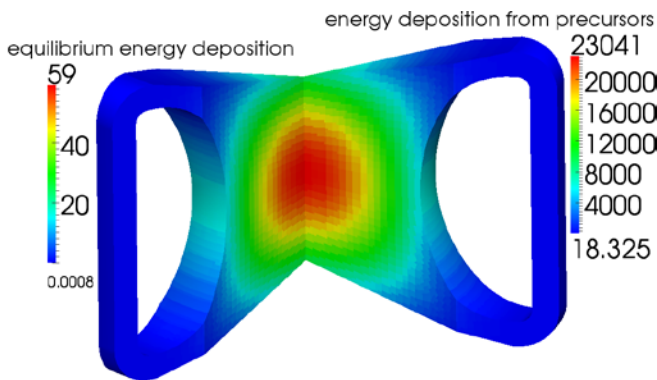


Figure 15: Energy deposition (MeV/source) calculated by MCNP mapped to OpenFOAM, equilibrium value (left) and calculated using (6) (right)

V. Conclusion

One key characteristic of a Molten Salt Reactor is the use of a flowing liquid fuel which also serves as coolant for heat transport from the core to the intermediate loop heat exchangers. The neutronics and thermohydraulics design of such a reactor have then some important differences with respect to nuclear power system using a solid fuel. In particular, some unique phenomena caused by the circulation of the liquid fuel in the reactor have to be integrated in the analysis. These phenomena include: the motion of the delayed neutron precursors, the reactor core wall temperature distribution, etc. Coupled neutronics and thermohydraulics numerical simulations have been realized at steady state conditions to adequately take into account these phenomena.

These preliminary numerical simulations are carried-out using the Monte Carlo code MCNP and the Computation Fluid Dynamic code OpenFOAM. A method as been developed to evaluate the numerical convergence of the Monte Carlo calculation for the neutron production and the energy deposition.

The developed tools take into account the effects of the precursor's motion. We have evaluated some reactor parameters such as the effective fraction of delayed neutrons, the energy deposition field including the effect of the temperature distribution, and the hot spot temperature on the wall.

Acknowledgment

The authors wish to thank the PACEN (Programme sur l'Aval du Cycle et l'Energie Nucléaire) and NEEDS (Nucléaire : Energie, Environnement, Déchets, Société) programs of the French Centre National de la Recherche Scientifique (CNRS), the IN2P3 department of CNRS, the European program EVOL (Evaluation and Viability of Liquid Fuel Fast Reactor System) of FP7, and the I-MEP2 Doctoral College of Grenoble University for their support.

References

- 1) Merle-Lucotte E., Heuer D. et al., "Minimizing the Fissile Inventory of the Molten Salt Fast Reactor", Proceedings of the Advances in Nuclear Fuel Management IV (ANFM 2009), Hilton Head Island, USA (2009)
- 2) Mathieu L., Heuer D., E. Merle-Lucotte, et al., "Possible Configurations for the Thorium Molten Salt Reactor and Advantages of the Fast Non-Moderated Version", *Nucl. Sc. and Eng.*, 161, 78-89 (2009)
- 3) Rubiolo P., Heuer D., E. Merle-Lucotte et al., "Overview and Perspectives of the Molten Fast Salt Reactor (MSFR) Concept", Proceedings of the Conference on Molten Salts in Nuclear technology (CMSNT-2013), Bhabha Atomic Research Centre, Mumbai, India (2013)
- 4) GIF (Generation IV International Forum), 2008, Annual report http://www.gen-4.org/PDFs/GIF_2008_Annual_Report.pdf, 36-41 (2008)
- 5) <http://www.openfoam.org/docs/>
- 6) <https://laws.lanl.gov/vhosts/mcnp.lanl.gov/mcnp5.shtml>
- 7) Delpech S., E. Merle-Lucotte, Heuer D. et al., "Reactor physics and reprocessing scheme for innovative molten salt reactor system", *J. of Fluorine Chemistry*, 130, Issue 1, 11-17 (2009)
- 8) Shih T.-H., Liou W. W., Shabbir A., Yang Z., and Zhu J., "A New k-epsilon Eddy-Viscosity Model for High Reynolds Number Turbulent Flows - Model Development and Validation", *Computers Fluids*, 24(3):227-238 (1995)
- 9) Ignatiev V., Feynberg O., Merzlyakov A. et al., "Progress in Development of MOSART Concept with Th Support", Proceedings of ICAPP 2012, Paper 12394, Chicago, USA (2012)
- 10) Vaiana F., "Couplage neutronique - thermohydraulique, Application au Réacteur à Neutrons Rapides refroidi à l'hélium", PhD Thesis, Institut Polytechnique de Grenoble (2009)
- 11) Rouch H., Geoffroy O., Heuer D. et al, "Preliminary Thermalhydraulic Core Design of a Molten Salt Fast Reactor", accepted in *Annals of Nuclear Energy* (2013)
- 12) Aufiero M., Brovchenko M., Cammi A. et al, "Calculating the effective delayed neutron fraction in the Molten Salt Fast Reactor : analytical, deterministic and Monte Carlo approaches", accepted in *Annals of Nuclear Energy* (2013)